Universiteit
Leiden
The Netherlands

The aorta in transposition of the great arteries

Palen, R.L.F. van der

Citation
Palen, R. L. F. van der. (2021, June 16). *The aorta in transposition of the great arteries*. Retrieved from https://hdl.handle.net/1887/3185513

Version:	Publisher's Version
License:	Licence agreement concerning inclusion of doctoral thesis in the Institutional Repository of the University of Leiden
Downloaded from:	https://hdl.handle.net/1887/3185513

Note: To cite this publication please use the final published version (if applicable).

Cover Page

Universiteit Leiden

Leiden University Repository

The handle http://hdl.handle.net/1887/3185513 holds various files of this Leiden University dissertation.

Author: Palen, R.L.F. van der
Title: The aorta in transposition of the great arteries
Issue date: 2021-06-16

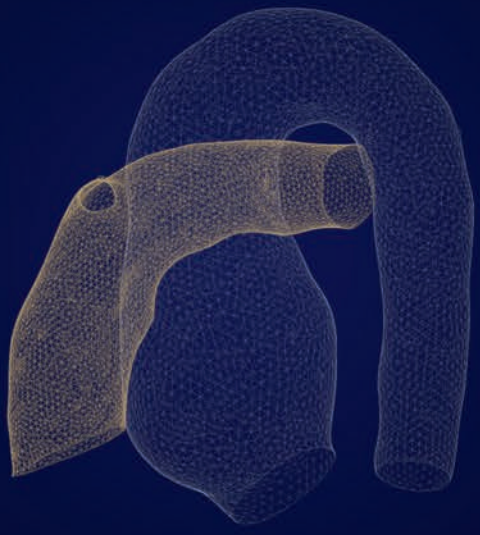

CHAPTER 7

Altered ascending aorta hemodynamics in patients after arterial switch operation for transposition of the great arteries

Journal of Magnetic Resonance Imaging. 2020;51:1105-16

Roel L.F. van der Palen
Quirine S. Deurvorst
Lucia J.M. Kroft
Pieter J. van den Boogaard
Mark G. Hazekamp
Nico A. Blom
Hildo J. Lamb
Jos J.M. Westenberg*
Arno A.W. Roest*

* shared last authorship

Abstract

Background
Patients with transposition of the great arteries (TGA) have an altered aortic geometry after an arterial switch operation (ASO), with neo-aortic root dilatation as an important complication. Geometry-related aortic hemodynamics have been assumed to contribute to pathology of the ascending aorta (AAo).

Purpose
To evaluate aortic flow displacement (FD) and regional wall shear stress (WSS) in relation to ascending neo-aortic geometry in children after ASO.

Study type
Prospective.

Population
Twenty-eight TGA patients after ASO and ten healthy volunteers.

Field Strength/Sequence
3.0T/4D flow (segmented fast-spoiled echo pulse), non-contrast enhanced MR angiography (Dixon), and anatomic images (SSFP).

Assessment
Aortic diameters and body surface area-indexed aortic dimensions (Z-scores), normalized FD and planar ascending aortic WSS.

Statistical tests
Mann Whitney and chi-square tests for differences in FD magnitude, WSS, and FD directionality between groups, respectively. Spearman rank correlation to assess the degree of association between aortic geometry, FD and WSS parameters. Shapiro-Wilk test to evaluate distribution normality on the absolute differences in octant location between FD and WSS.

Results
TGA patients showed a significantly dilated proximal AAo and relatively small mid-AAo dimensions at the level of the pulmonary arteries (Z-scores neo-aortic root: 4.38 ± 1.96 vs 1.52 ± 0.70, $P < 0.001$; sinotubular junction: 3.48 ± 2.67 vs 1.38 ± 1.30, $P = 0.010$; mid-AAo: 0.32 ± 3.06 vs 1.69 ± 1.24, $P = 0.001$). FD magnitude was higher in TGA patients (neo-aortic root: 0.048 ± 0.027 vs 0.021 ± 0.006, $P < 0.001$; sinotubular junction: 0.054 ± 0.037 vs 0.029 ± 0.013, $P < 0.05$) and was related to the neo-aortic Z-score. Clear areas of higher WSS at the right and anterior aortic wall regions along the distal AAo were detected in TGA patients, most pronounced in those with relatively smaller mid-AAo diameters.

Data conclusion
TGA-specific geometry related to the ASO, evidenced by neo-aortic root dilatation and a sudden change in vessel diameter at mid-AAo level, leads to more aortic flow asymmetry in the proximal AAo and WSS distribution with higher WSS at the right and anterior aortic wall regions along the distal AAo.

Introduction

The arterial switch operation (ASO) is currently the operation of choice for patients with transposition of the great arteries (TGA).[1] The ASO replaced the atrial switch operation with excellent early and long-term survival and good function outcome in most of the patients. However, studies on large cohorts of patients show progressive neo-aortic root dilatation over time with an associated increased incidence of neo-aortic regurgitation and the need for root and/or valve re-operation.[2, 3] Factors involved in the pathophysiological mechanisms for neo-aortic root dilatation are largely unknown.

The ASO with the Lecompte maneuver restores ventriculo-arterial concordance; however, the spatial relation between the aorta and pulmonary artery is still abnormal, with the pulmonary trunk situated anterior to the ascending aorta and the two pulmonary arteries embracing the ascending aorta. During the ASO, the aorta and pulmonary trunk are transected just above the commissures and relocated, leaving the semilunar valves and native root in its original position. Subsequently, the proximal part of the native pulmonary trunk becomes the proximal neo-aorta and the native aortic root becomes the neo-pulmonary root. The arterial relocation leads to an abnormal angulation between the neo-aortic valve and the newly formed sinotubular junction (STJ) in TGA patients compared with healthy subjects, and geometric alterations in the ascending neo-aorta after ASO have hemodynamic consequences.[4, 5]

Currently, 4D flow magnetic resonance imaging (4D flow MRI) allows visualization and quantification of abnormal hemodynamics within the ascending aorta[6] which has led to better knowledge of cardiovascular hemodynamics and disease progression in patients with congenital heart disease-related aortopathy.[7-11] Different studies have shown that aortic flow eccentricity, defined as the displacement of peak systolic flow from the aortic center, is related to aortic morphology in bicuspid valve-related dilated aortopathy.[11, 12] Another comprehensive hemodynamic parameter that can be derived from 4D flow MRI is wall shear stress (WSS). WSS is defined as the viscous shear force of flowing blood acting tangentially to the vessel wall. Areas of high WSS have been associated with marked histological changes in the ascending aortic vessel wall in patients with bicuspid aortic valves.[13] In addition, abnormal WSS has been suggested to have potentially contributing effects on vessel dilatation and aneurysm formation; for example, on the thoracic aorta and on intracranial aneurysms.[14, 15] In TGA patients after ASO, abnormal flow patterns in the ascending aorta are present in the majority of patients.[4] Assessment of aortic flow displacement and

detection of areas of high WSS may be helpful in unravelling flow alterations and their relationship with altered arterial geometry and aortic dilatation. We hypothesized that the specific geometry of the ascending neo-aorta after ASO including the Lecompte maneuver is related to altered ascending aortic flow hemodynamics. Therefore, the aim of this study was to evaluate aortic flow displacement and regional WSS in relation to ascending neo-aortic geometry in patients after ASO for TGA.

Materials and methods

Study population

All patients or their legal guardians and all healthy subjects gave written informed consent for the study. The study protocol was approved by the institutional Medical Ethical Committee. Twenty-eight patients with simple TGA or TGA with ventricular septal defect (VSD) were included in this study between December 2015 and March 2018. TGA patients (simple TGA or TGA with VSD) aged 10-25 years that underwent regular MRI examinations of the heart and large vessels as part of the standardized clinical follow-up protocol for early detection of well-known sequelae after ASO (typically performed shortly after birth) were asked for participation in the study. Aortic 4D flow acquisitions were performed additionally to a standard-of-care cardiac MRI. To ensure morphologic homogeneity, patients with complex TGA including Taussig-Bing anomaly, prior left ventricular outflow tract obstruction, bicuspid neo-aortic valve, aortic arch obstruction, moderate-to-severe neo-aortic insufficiency, or prior neo-aortic valve or root re-operations were not included in the study. All patients underwent 4D flow MRI in addition to the clinically indicated standard-of-care MRI assessment of the heart and large vessels. Ten healthy subjects with a tricuspid aortic valve and without history of cardiovascular disease were included as a healthy reference group. All healthy subjects underwent the same MRI assessment of the heart and great vessels including 4D flow aortic imaging as part of a validation study.[16]

MRI acquisition

MRI examinations including aortic 4D flow imaging of all patients and healthy subjects were performed at the same 3T scanner (Ingenia, Philips Medical Systems, the Netherlands; Software Stream 4.1.3.0) using a combination of FlexCoverage Posterior coil in the table top with a dStream Torso coil, providing up to 32 coil elements for signal reception. The standard-of-care MRI exam of the heart and large vessels included dynamic ECG gated two-dimensional (2D) cine steady state free precession (SSFP) imaging for the evaluation of cardiac anatomy and function, as well as a non-contrast enhanced three-dimensional (3D) free-breathing navigator-gated MR angiography (NCE-MRA) images for the assessment of thoracic aorta diameters.[17] For the NCE-MRA imaging, a Dixon sequence with prospective triggering and gated to end diastole, respiratory navigator gating was used with following sequence parameters: spatial resolution = 1.6 x 1.6 x 3.2 mm, echo time/repetition time = 2.3/3.6-3.9

msec, field of view = 300 x 300 x 99 mm; reconstructed voxel size = 0.8 x 0.8 x 1.6 mm. 4D flow MRI was a segmented fast spoiled-gradient echo technique with standard 4-point velocity encoding in all three directions. The 4D flow MRI was acquired during free breathing using a hemidiaphragm respiratory navigator and retrospective ECG gating. Scan parameters were as follows: velocity-encoding of 200-300 cm/s in three directions, acquired spatial resolution = 2.5 x 2.5 x 2.5 mm, temporal resolution = 33.6-36.8 msec, echo time/repetition time = 2.4-2.7/4.2-4.6 msec, flip angle = 10°, field of view = 350 x 250 x 75 mm, segmentation factor = 2, sensitivity encoding (SENSE) was used with SENSE factor 2.5 in anterior-posterior direction. Acquisition time was on average 12 minutes. Concomitant gradient correction and initial phase offset correction was performed from standard available scanner software.

Data analysis

Aortic dimensions and cardiac function

Left ventricular ejection fraction was measured from short-axis SSFP images by a radiologist with over 20 years of experience in MR imaging (L.K.). From NCE-MRA, ascending aortic diameters were measured at five standardized anatomic landmarks according to international guidelines,[18] consisting of the neo-aortic valve (AoV), neo-aortic root (Root), STJ, for TGA patients defined as the aortic level 5-7 mm below the pulmonary artery bifurcation; mid-ascending aorta at the level of the pulmonary artery bifurcation (mid-AAo) and the distal ascending aorta, just proximal to the origin of the brachiocephalic trunk (AAo-BCT) (Figure 1). All diameters were measured from edge to edge and obtained from a sagittal-axis orientation. The mean neo-aortic root diameters (i.e. average of three cusp-to-commissure diameters) were measured perpendicular to the aortic axis on NCE-MRA double oblique transversal angulated multiplanar reconstructions. A second observer (independent radiologist with 10 years of experience in cardiovascular MR imaging) remeasured all ascending aortic diameters in a random subset of healthy volunteers (n = 5) and patients (n = 10) to assess interobserver reproducibility. To take into account differences in age and body size between individuals, aortic Z-scores were determined for each individual using MRI-derived normative data of aortic diameters in children and adolescents.[19] Body surface area was calculated using the Mosteller formula. The Z-score represents the deviation of a given measurement to the body size or age-specific population mean. A Z-score between -2 and +2 is considered normal. Aortic diameter ratio between the neo-aortic root diameter and the mid-AAo diameter was calculated for each subject $\left(\frac{\text{Root}}{\text{mid-AAo}}\right)$.

4D Flow - Aortic flow displacement & WSS assessment

4D flow MRI data were imported into the software program CAAS MR 4D flow v2.0 (Pie Medical Imaging BV, Maastricht, the Netherlands). Additional phase offset correction and antialiasing was performed in the CAAS MR software package. The 4D flow segmentation was performed as previously described.[16] In short, from the 4D flow raw data (Figure 1A) the peak systolic phase was automatically detected by the CAAS MR Flow software program by identification of the cardiac phase with the highest variance in the 3D velocity dataset.

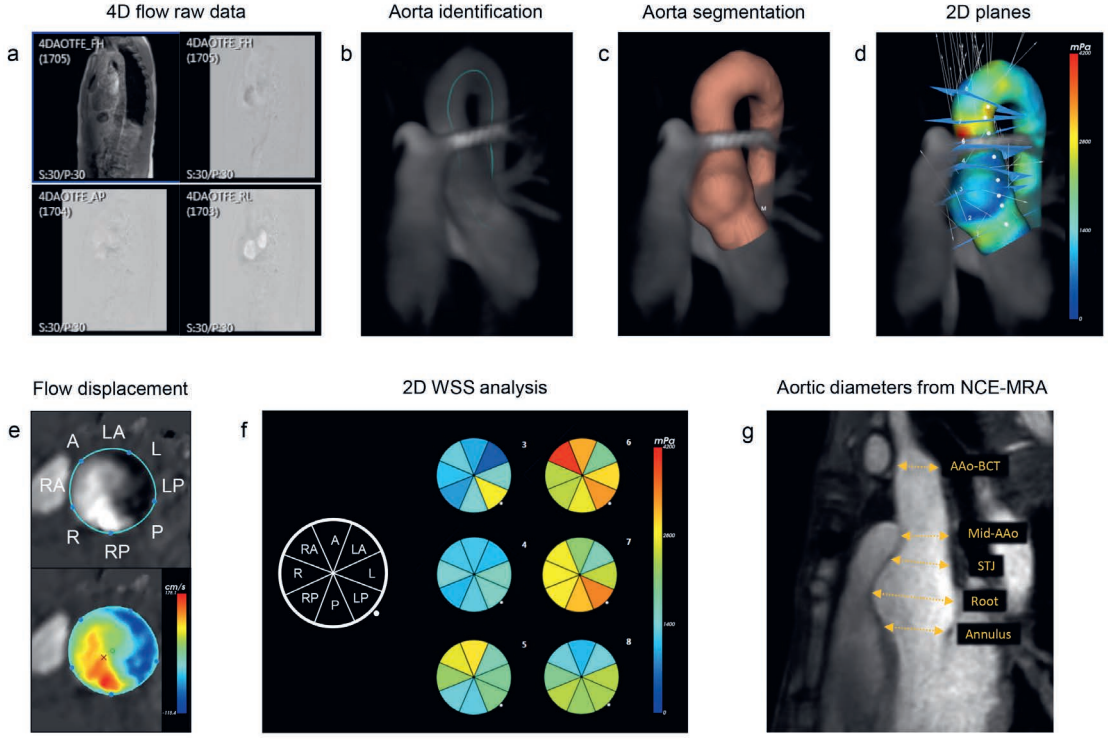

Figure 1. Measurement of aortic diameters and workflow 4D flow analysis for flow displacement and wall shear stress.
4D flow dataset (A). Identification of the thoracic aorta and automatic computation of aortic centerline (B). 3D segmentation of the thoracic aorta (C). Positioning of eight cross-sectional planes perpendicular to the centerline: 1. left ventricular outflow tract, 2. aortic valve, 3. neo-aortic root, 4. sinotubular junction, 5. mid-ascending aorta, 6. distal ascending aorta-1 (dAAo-1), 7. distal ascending aorta-2 (dAAo-2), 8. proximal to the origin of the brachiocephalic trunk (D). Determining flow displacement and direction, O = center of vessel, × = center of velocity (E). Planar 2D WSS analysis (F). Aortic diameter measurements from non-contrast enhanced magnetic resonance angiography (G). AAo-BCT, distal ascending aorta proximal to the origin of the brachiocephalic trunk; A, anterior; LA, left-anterior; L, left; LP, left-posterior; mid-AAo, mid-ascending aorta; NCE-MRA, non-contrast enhanced magnetic resonance angiography; P, posterior; RP, right-posterior; R, right; RA, right-anterior; Root, neo-aortic root; STJ, sinotubular junction; WSS, wall shear stress.

For this phase (Figure 1B), the segmentation was initialized by manually placing two points (start and endpoint): one in the left ventricular outflow tract and one in the descending aorta, at the same level as the start point (Figure 1B). A centerline was automatically created (Figure 1B) and a phase-specific 3D aortic volume was automatically segmented for this peak systolic phase (Figure 1C) plus two consecutive phases before and two phases after this peak systolic phase. For the ascending aorta, the peak systolic 3D aortic segmentation was selected, visually checked and manually adapted when necessary in case of segmentation incorrectness. Eight cross-sectional planes were manually positioned along the ascending aorta perpendicular to the centerline (Figure 1D). The 2D analysis planes were placed from the LVOT to the origin of the brachiocephalic trunk at anatomic locations: 1. left ventricular outflow tract (LVOT), 0.5 cm beneath the neo-aortic valve (AoV) level; 2. AoV; 3. neo-aortic root (Root); 4. STJ, for TGA patients defined as the aortic level 5-7 mm below the pulmonary artery bifurcation; 5. mid-AAo, at the level of the pulmonary artery bifurcation; 6. distal ascending aorta-1 (dAAo-1), at 1/3 distance between plane 5 and plane 8, calculated from plane 5; 7. distal ascending aorta-2 (dAAo-2), at 2/3 distance between plane 5 and plane 8, calculated from plane 5; 8. proximal to the origin of the brachiocephalic trunk (AAo-BCT) (Figure 1D).

Normalized systolic flow displacement (FD) was calculated in each of the cross-sectional planes according to a method previously described by Sigovan et al.[20] (Figure 1E). Briefly, FD is defined as the distance between the anatomical center of the vessel and the center velocity (Cvel) of the flow at peak systole, normalized to the vessel lumen diameter. The vessel lumen diameter was automatically identified on 2D analysis planes by the CAAS MR software and manual delineation of the vessel lumen boundary was performed with the available adaptation tool from the software in case of incorrectness. To determine the center of velocity the next equation was used:

$$C_{vel,j} = \frac{\sum_i r_{i,j}|v_i|}{\sum_i |v_i|}, i = lumen\ pixels; j = x, y, z\ positions; v_i = velocity$$

The vessel circumference was divided into eight equally-sized segments (octants) and for each patient the direction of FD in each cross-sectional plane was qualitatively assessed (A = anterior, LA = left-anterior, L = left, LP = left-posterior, P = posterior, RP = right-posterior, R = right, RA = right-anterior) (Figure 1E).

Peak systolic WSS was calculated for eight aortic wall segments from the cross-sectional planes 3-8 (i.e. from the neo-aortic root to the origin of the brachiocephalic trunk) (Figure 1F). The systolic WSS was calculated based on the extracted velocity profile perpendicular to the phase-specific 3D aortic surface. After factorizing the velocity profile into its component parallel to the aortic lumen wall, the systolic WSS was computed by the first derivative of a quadratic approximation of that velocity profile at the location of the aortic lumen wall.[16]

Similarities between the location of FD and the location of the highest systolic WSS were evaluated by determining the absolute difference between these locations. The number of octant positions clockwise or counterclockwise away from the position of the FD location

was calculated and categorized as follow: 0 = no difference in location; 1 = difference of 1 octant position; 2 = difference of 2 octant positions; 3 = difference of 3 octant positions; 4 = difference of 4 octant positions. A difference ≤1 octant position was defined as good to excellent. In case of no relationship, a Gaussian (nonskewed) distribution of the absolute differences is expected, with a nonsignificant result from the normality test.

Statistical analysis

Statistical analyses were performed using IBM SPSS Statistics version 23 (IBM, Chicago, IL, USA). Variables are presented as mean ± standard deviation or median [interquartile range, IQR] if not normally distributed. A Shapiro-Wilk test was used to test variables for normal distribution. A chi-square test was performed to investigate differences in gender distribution between TGA patients and healthy subjects. To compare normally distributed parameters between TGA patients and healthy subjects an unpaired *t*-test was used. An interobserver reproducibility analysis was performed for the aortic diameter measurements. For comparison of differences in magnitude of FD and regional aortic WSS between the TGA patients and healthy subjects a Mann Whitney test was used. A chi-square test was performed to investigate differences in FD directionality between TGA patients and healthy subjects and within the TGA patients based on the preoperative spatial position of the great arteries. The relationship between aortic Z-score and FD was investigated using correlation analysis based on linear regression (Spearman's correlation). Correlation analysis based on linear regression (Spearman's correlation) was also performed to assess the effect of aortic geometry (aortic diameter ratio between neo-aortic root and mid-AAo) and WSS parameters. To evaluate distribution normality on the absolute differences in octant location between flow displacement in root, STJ and mid-AAo and location of highest peak systolic WSS at mid-AAo level, a Shapiro-Wilk test was performed and skewness and kurtosis markers were calculated. $P < 0.05$ was considered significant for all statistical tests. A Bonferroni correction was performed to adjust for the multiple comparisons for the planar WSS analysis along the AAo and differences between groups were considered significant for $P < 0.00104$.

Results

Baseline and surgical characteristics are presented in Table 1. No significant differences between TGA patients and healthy subjects were observed except for age. All patients and healthy subjects had a normal systolic left ventricular function. The proximal ascending aorta in TGA patients, including the indexed neo-aortic valve annulus, neo-aortic root and STJ, was significantly larger and dilated compared with healthy subjects. Using a Z-score >2.0 to define aortic dilatation, 25 patients (89%) had neo-aortic root dilatation and 19 of the TGA patients (68%) had dilatation of the STJ. In contrast, the diameter of the mid-AAo, the location where the pulmonary arteries embrace the ascending aorta from anterior in TGA patients, was significantly smaller in TGA patients compared with healthy subjects (mid-AAo: 17.0 [16.0-18.3] vs 20.5 [18.0-21.6] mm/m^2, $P = 0.001$; mid-AAo Z-score 0.32 ± 3.06

Table 1. Baseline characteristics and MRI measurements

	TGA patients (*n* = 28)	Healthy subjects (*n* = 10)	*P* value
Patient and surgical characteristics			
Male, *n* (%)	18 (64.3)	5 (50.0)	0.473
Age, years	16.0 ± 3.3	27.3 [24.9-28.4]	<0.001
Weight, kg	60.5 ± 14.0	68.3 ± 12.7	0.129
Height, cm	170.8 ± 12.2	175.6 ± 6.6	0.250
Body surface area, m^2	1.7 ± 0.2	1.8 ± 0.2	0.137
LV ejection fraction, %	59.1 ± 5.7	62.0 ± 2.5	0.155
Surgical variables			
Age at ASO, days	6.0 [4.0-10.0]		
Weight at ASO, kg	3.5 ± 0.5		
Lecompte maneuver, *n* (%)	28 (100)		
Transposition type, *n* (%)			
TGA-IVS	21 (75.0)		
TGA-VSD	7 (25.0)		
Great artery position, *n* (%)			
Aorta right anterior to PA	15 (53.6)		
Aorta right side to PA	3 (10.7)		
Aorta anterior to PA	7 (25.0)		
Aorta left anterior to PA	3 (10.7)		
Aortic diameters (mm/ $BSA^{0.5}$)[a]			
Neo-aortic valve annulus	18.8 [17.4-20.1]	15.2 [13.9-17.4]	<0.001
Neo-aortic root sagittal	28.0 [25.7-29.7]	23.1 [21.0-24.2]	<0.001
Neo-aortic root short-axis, mean	27.2 [26.3-30.6]	22.4 [21.5-22.9]	<0.001
Sinotubular junction	20.6 [19.7-24.0]	19.2 [17.2-20.2]	0.008
Mid ascending aorta	17.0 [16.0-18.3]	20.5 [18.0-21.6]	0.001
Origin of BCT	17.2 [15.5-18.1]	18.0 [16.3-18.9]	0.142
Aortic Z-scores[b]			
Neo-aortic root short-axis, mean	4.38 ± 1.96	1.52 ± 0.70	<0.001
Sinotubular junction	3.48 ± 2.67	1.38 ± 1.30	0.010
Mid ascending aorta	0.32 ± 3.06	1.69 ± 1.24	0.001
Origin of BCT	-0.52 ± 1.21	0.20 ± 1.29	0.122

[a] Data are presented as median [interquartile range]. [b] Data are presented as mean ± SD.
ASO, arterial switch operation; BCT, brachiocephalic trunk; BSA, body surface area; IVS, intact ventricular septum; LV, left ventricular; PA, pulmonary artery; TGA, transposition of the great arteries; VSD, ventricular septal defect.

vs 1.69 ± 1.24, *P* = 0.001). The interobserver reproducibility analysis showed an excellent agreement between the aortic measurements of the observers: mean difference 0.18 mm, limits of agreement (±2 SD) of 3.9 mm; coefficient of variation 3.2%; intraclass correlation coefficient: 0.979 (95% confidence interval [CI] 0.969-0.986); correlation: r = 0.96, *P* < 0.001.

Aortic flow displacement

The group-averaged magnitude of FD along the entire ascending aorta for both TGA patients and healthy subjects is illustrated in Figure 2. Flow displacement magnitude was significantly higher in TGA patients compared with the healthy subjects at the level of the neo-aortic root (FD 0.048 ± 0.027 vs 0.021 ± 0.006, *P* < 0.001) and STJ (FD 0.054 ± 0.037 vs 0.029 ± 0.013, *P* < 0.05). No differences in FD magnitude were found at the mid-AAo level (TGA vs healthy subjects: FD 0.050 ± 0.034 vs 0.033 ± 0.021, *P* = 0.083).

Flow displacement direction and magnitude for all individual patients and healthy subjects were depicted for three adjacent aortic planes (root, STJ, and mid-AAo) in Figure 3. The FD direction in the ascending neo-aorta in TGA patients (root and mid-AAo) was different compared with healthy subjects (Figure 3; Root *P* = 0.024, mid-AAo *P* = 0.002).

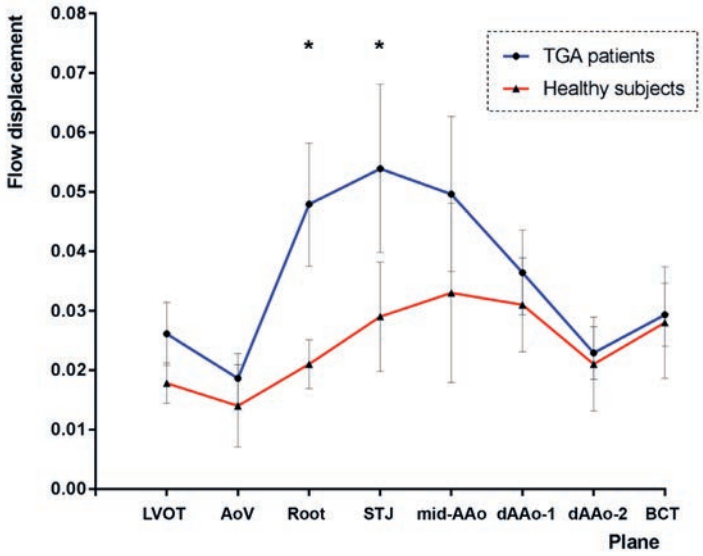

Figure 2. Flow displacement along the ascending aorta.
Group averaged flow displacement along the ascending aorta (mean, 95% CI) at aortic levels as stated in Figure 1D. * *P* < 0.05.
AoV, neo-aortic valve; BCT, distal ascending aorta proximal to the origin of the brachiocephalic trunk; dAAo-1, distal ascending aorta at 1/3 distance between 'mid-AAo plane' and 'BCT plane'; dAAo-2, distal ascending aorta at 2/3 distance between 'mid-AAo plane' and 'BCT plane'; LVOT, left ventricular outflow tract; mid-AAo, mid ascending aorta; Root, neo-aortic root; STJ, sinotubular junction.

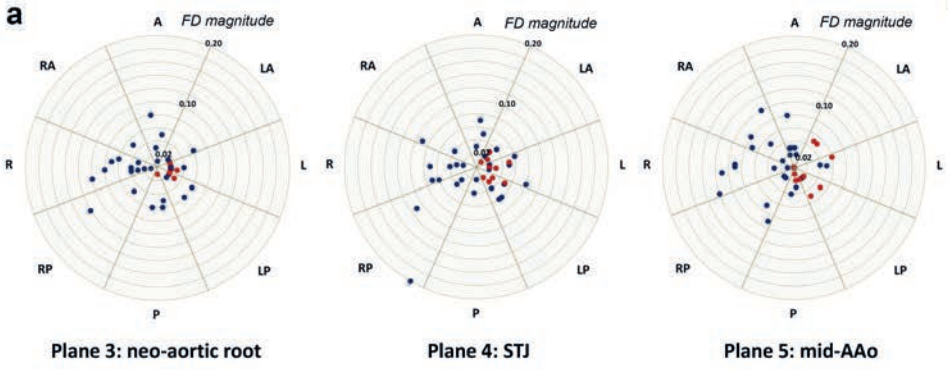

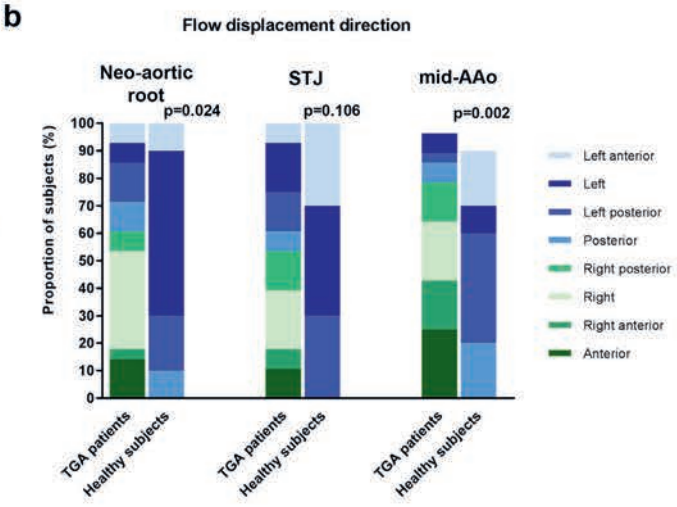

Figure 3. Flow displacement magnitude and direction profiles.
Each dot represents the peak systolic flow displacement direction (i.e. octant location) and magnitude per subject (i.e. FD magnitude increasing from inner (0) to outer circle (0.20)): TGA patients (blue dots), healthy subjects (red dots) (A). Flow displacement direction per octant in TGA patients (n = 28) vs healthy subjects (n = 10) (B). Of note, FD direction analysis for the mid-AAo plane is presented for 27 TGA patients and nine healthy subjects because of no FD in two subjects, one in each group.
FD, normalized flow displacement; mid-AAo, mid-ascending aorta; STJ, sinotubular junction; TGA, transposition of the great arteries.

Healthy subjects showed a primarily central and central-left orientated (left-anterior, left or left-posterior) aortic flow at the root, STJ and mid-AAo levels, whereas the TGA patients showed a more heterogeneous flow direction, both left- and rightward orientated in the root that shifted more to anterior and right side from root to the mid-AAo (Figure 3). Differences in FD direction between TGA patient subgroups based on preoperative great artery position were observed in the neo-aortic root (Figure 4). TGA patients with a right-anterior or right-sided position of the aorta related to the pulmonary artery (n = 18) showed more FD to the right-side of the AAo, whereas a left-anterior or anterior position of the aorta (n = 10) resulted in more FD to the left-side of the aortic wall at the level of the neo-aortic root (P = 0.025) (Figure 4). At the level of the STJ and mid-AAo this difference in FD direction could not be statistically detected (STJ, P = 0.148; mid-AAo, P = 0.738).

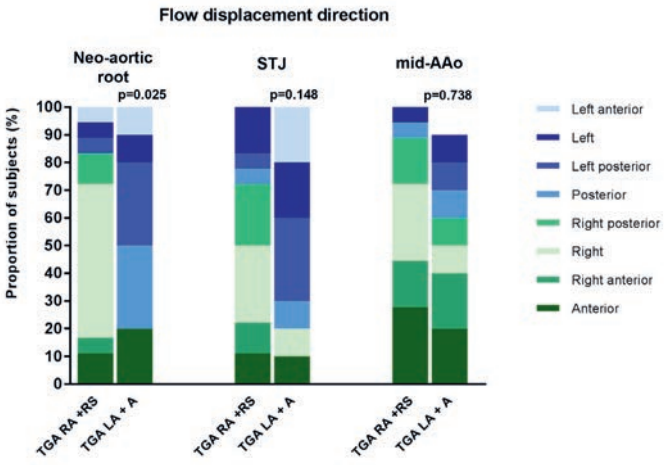

Figure 4. Flow displacement direction per octant in TGA subgroups.
TGA patients are divided into subgroups based on great artery position before arterial switch operation (aorta related to pulmonary trunk). Group 1 (TGA RA + RS) consists of TGA patients with the aorta right-anterior (RA) or right-sided (RS) to the pulmonary trunk (n = 18). Group 2 (TGA LA + A) consists of TGA patients with the aorta anterior (A) or left-anterior (LA) to the pulmonary trunk (n = 10). Of note, FD direction for the mid-AAo plane is presented in nine TGA LA+A patients because of no FD in 1 TGA LA+A patient.
A, anterior; LA, left-anterior; RA, right anterior; RS, right-sided; TGA, transposition of the great arteries.

Ascending aortic WSS assessment

The systolic WSS distribution along the ascending aorta showed distinct differences between the TGA patients and the healthy subjects. In the proximal ascending aortic segment (plane 3-4: root and STJ) the systolic WSS in the TGA patients was evenly distributed along the circumference of the aortic wall and WSS was low. In specific regions at these levels (root and STJ) significantly lower WSS was found compared with the healthy subjects (Figure 5, plane 3-4: root and STJ).

In TGA patients, significantly higher and highly asymmetric peak systolic WSS was detected in the distal ascending aortic segments, at and beyond the level of the embracement of the ascending aorta by the pulmonary artery branches (plane 6-8: dAAo-1, dAAo-2, and AAo-BCT) (Figure 5). At these distal AAo planes, the distribution of the systolic WSS in the TGA patients was uneven, with the most pronounced significantly increased peak systolic WSS in the anterior regions (right-anterior, anterior and left-anterior, $P \leq 0.001$). In healthy subjects there was no increase in systolic WSS in the distal part of the ascending aorta (Figure 5).

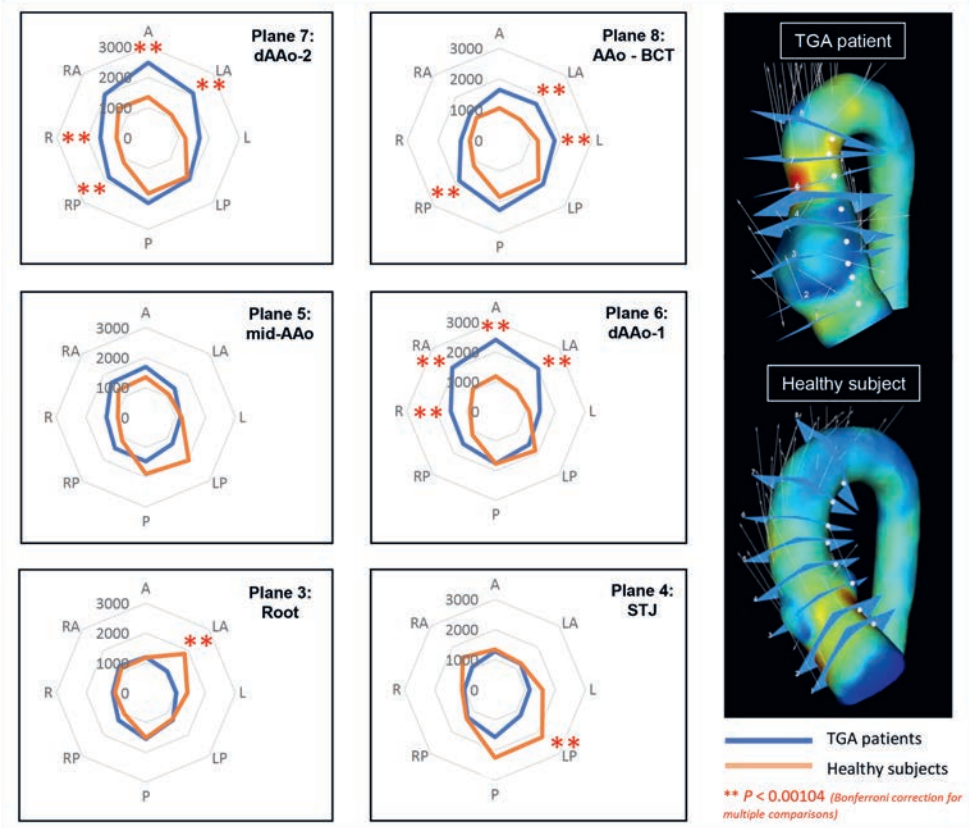

Figure 5. Planar aortic WSS assessment along the ascending aorta in TGA patients and healthy subjects.
Wall shear stress in mPa. Mann Whitney test for comparison of differences in regional aortic WSS between the TGA patients and healthy subjects. Differences between the groups were considered significant for $P <$ 0.00104 (Bonferroni correction for multiple comparisons).
AAo-BCT, distal ascending aorta proximal to the origin of the brachiocephalic trunk; dAAo-1, distal ascending aorta at 1/3 distance between plane 5 'mid-AAo' and plane 8 'AAo-BCT'; dAAo-2, distal ascending aorta at 2/3 distance between plane 5 'mid-AAo' and plane 8 'AAo-BCT'; mid-AAo, mid ascending aorta; Root, neo-aortic root; STJ, sinotubular junction; TGA, transposition of the great arteries.

Flow displacement, WSS and correlations with aortic geometry

In the entire study cohort (TGA patients and healthy subjects), FD magnitude showed a moderate positive linear relationship with the neo-aortic Z-score at the level of the neo-aortic root and STJ (r = 0.54, $P < 0.001$ and r = 0.54, $P < 0.001$, respectively; Figure 6).

The octant location of FD in the root, STJ, and mid-AAo matched the location of maximum systolic WSS at mid-AAo level. The distribution of absolute differences in FD location (root, STJ, and mid-AAo) vs WSS location at mid-AAo level was skewed. In approximately 60% of the TGA patients, absolute differences in location between FD and WSS were 0 or 1 octant, representing no differences (Figure 7). TGA patients showed a predominant FD direction in the anterior and rightward orientation (right, right-anterior, anterior) from root to mid-AAo plane levels with elevated maximum systolic WSS in the anterior to right anterior locations from the mid- to distal AAo planes (Figure 3 and 7A). Wall shear stress magnitude in the distal ascending aortic planes showed a moderate positive linear relationship with the change in aortic dimension between the root and mid-AAo in TGA patients (Figure 8). A more pronounced increase in peak systolic WSS in those regions was detected in the patients with relatively small mid-AAo diameter compared with the neo-aortic root. The association between WSS magnitude and vessel diameter change was found for the right, right-anterior and anterior regions from the distal AAo planes (dAAo-1 and dAAo-2) (Figure 8), which corresponds with the regions where TGA patients showed highly asymmetric and elevated peak systolic WSS.

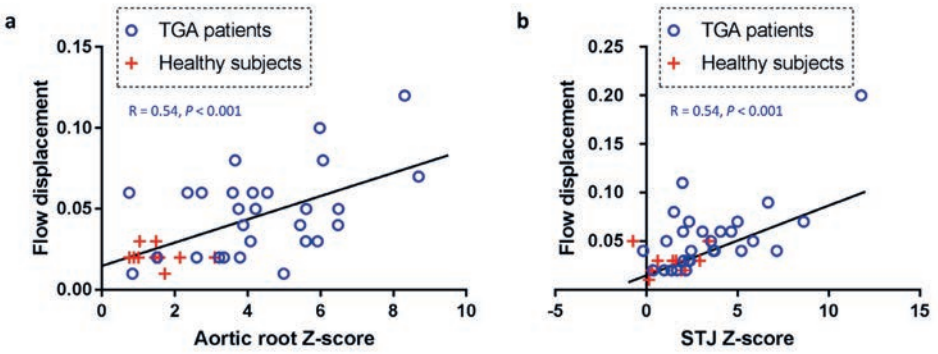

Figure 6. Relationship between aortic Z-score and normalized flow displacement in the proximal ascending aorta.
Aortic root: Z-score vs FD (A). STJ: Z-score vs FD (B).
STJ, sinotubular junction; TGA, transposition of the great arteries.

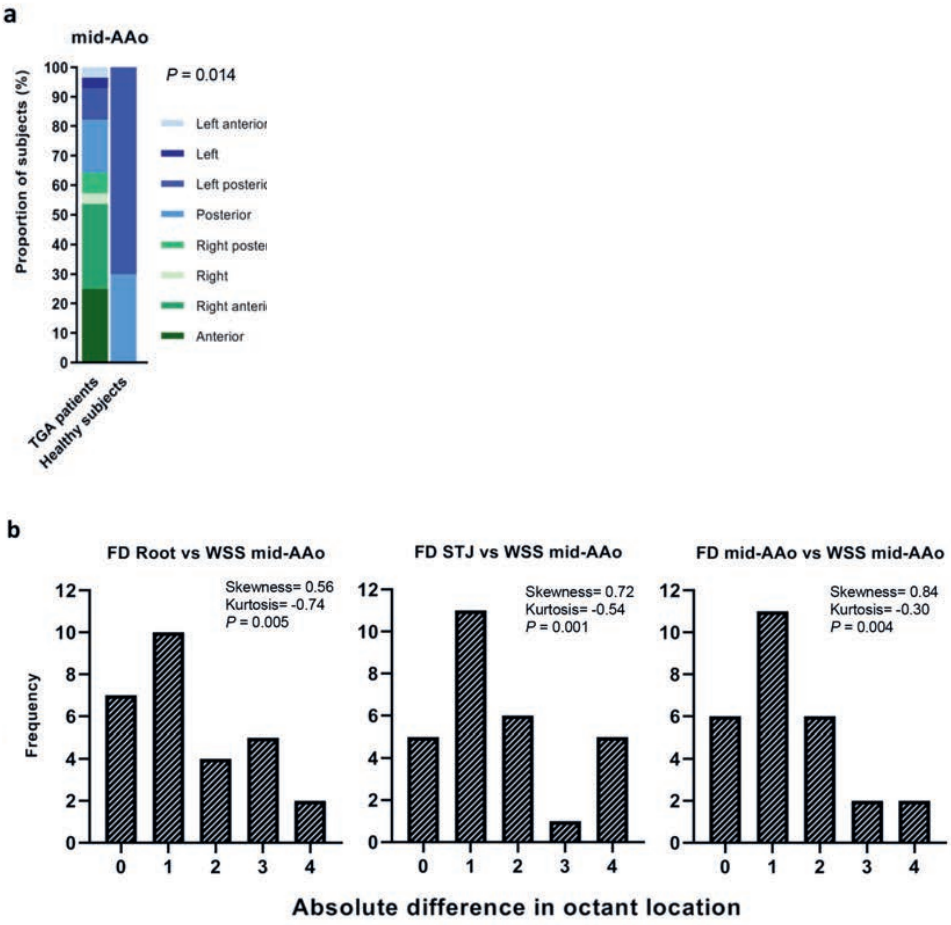

Figure 7. Location of peak systolic WSS (mid-AAo) and the relation with flow displacement direction in the proximal ascending aorta.
Location of peak systolic WSS at mid-AAo level in TGA patients and healthy subjects (A). Frequency histograms on the distribution of the absolute differences in octant location between FD (root, STJ, and mid-AAo) and the location peak systolic WSS (mid-AAo) in TGA patients (B). Normality tested by Shapiro-Wilk test. Of note, absolute differences in octant location between FD and WSS at the mid-AAo are presented for 27 TGA patients because of no FD in one TGA patient.
FD, normalized flow displacement; mid-AAo, mid-ascending aorta; Root, neo-aortic root; STJ, sinotubular junction; TGA, transposition of the great arteries; WSS, wall shear stress.

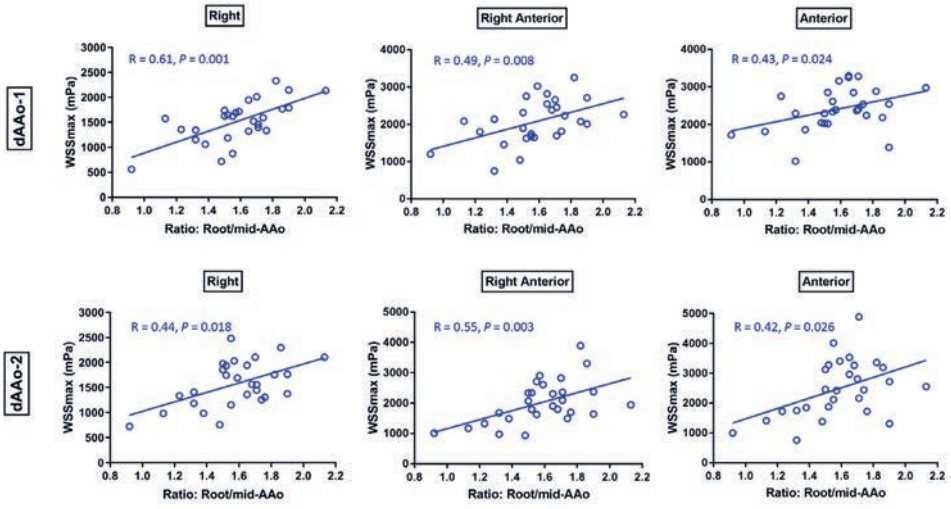

Figure 8. Relationship between aortic diameter change and wall shear stress along the distal ascending aorta. Diameter change between neo-aortic root and mid-ascending aorta represented as Root/mid-AAo ratio. Peak systolic wall shear stress (WSSmax) for the right, right-anterior and anterior regions along the distal ascending aorta (cross-sectional plane 6: dAAo-1 and plane 7: dAAo-2, as illustrated in Figure 1D).

Discussion

The results of this study demonstrate a more eccentric aortic flow in the proximal ascending aorta in TGA patients compared with healthy subjects. TGA-specific preoperative position of the great arteries showed different directionality of the eccentric flow profiles and the magnitude of the eccentric flow was linearly related with the local aortic Z-scores. The ASO-specific geometry consisted of neo-aortic root dilatation and a sudden change in vessel diameter at mid-ascending aortic level, the level of anterior aortic compression by the pulmonary trunk. This sudden change in aortic diameter was associated with increased and asymmetric peak systolic WSS distribution along the distal ascending aorta, most pronounced in the right and anterior aortic wall regions (right, right-anterior and anterior regions). The flow displacement direction from root to mid-AAo also corresponded to the peak systolic WSS distribution in the mid-AAo, but the contribution of FD on WSS distribution more upstream in the distal AAo was less compared with the effect of vessel tapering. The regions of abnormal increased WSS in the distal AAo clinically correlates with the location of the paper-thin and fragile anterior wall of the AAo that has been found in ASO patients during root reoperations.[21, 22]

Neo-aortic root dilatation is a key problem in long-term follow-up in patients after ASO for TGA because of its ongoing progression beyond the age of 18 years.[2, 3, 23] The neo-aortic root after ASO dilates and elongates and the STJ becomes more distally-displaced over time.[24] Similar to previous findings,[2, 5] the geometric alterations in the proximal ascending

aorta with neo-aortic root dilatation were accompanied by the relatively narrow mid-ascending aortic segments in this study, due to the anterior impression of the ascending aorta by the pulmonary trunk following Lecompte maneuver.

Mechanisms leading to progressive dilatation and elongation are not fully understood. Based on unoperated heart specimen with TGA, it is suggested that the arterial root in TGA patients has a diminished amount and altered distribution of collagen and that the root and left-sided semilunar valve are less firmly embedded in the myocardium,[25] which potentially makes the arterial root of these patients more susceptible for aortic dilatation after ASO. Semilunar valve diameters in TGA fetus are proven to be larger than in normal fetal hearts and the prenatal pulmonary valve size has been associated with neo-aortic root dilatation in the first years post-ASO.[26] Furthermore, it is known that abnormal blood flow may affect vessel wall tissue and may impact neo-aortic root dilatation as well.[13] Hemodynamic factors derived from 4D flow MRI, including flow eccentricity and WSS, have been associated with aortic diameter progression and vascular wall remodeling in patients with bicuspid aortic valve related aortopathy respectively.[12, 13] This study shows that children and adolescent TGA patients after ASO have an eccentric systolic flow in the ascending aorta: regions of most prominent flow eccentricity were detected at the level of the neo-aortic root and STJ. Consistent with the results of studies in patients with a bicuspid aortic valve,[12, 27] we found a close linear relationship between aortic dimensions and the normalized FD. In one of these studies, systolic FD was correlated with future ascending aortic growth in patients with bicuspid valve anatomy.[12] Despite the correlations found in this and other studies, longitudinal studies in patients after ASO are needed to assess the causative role of systolic FD for progressive neo-aortic root dilatation. Furthermore, the TGA-specific preoperative spatial position of the great arteries showed to be a factor for different directionality of the eccentric flow profiles in the neo-aortic root. Most likely this is the result of a different angulation between the neo-aortic valve and the newly formed STJ, depending on the location from where the aorta needs to be transposed on top of the neo-aortic root, stressing the influence of geometry on flow deviation within the ascending aorta. Next to this, a cardiac MRI study showed that a more acute aortic arch angulation, as is typical in post-ASO aortic geometry, is a risk factor for the development of root dilatation and valve regurgitation.[28]

A comparative computational fluid dynamic (CFD) and *in vitro* 4D flow MRI phantom study on the thoracic aorta from a single TGA case after ASO supports the findings of our study.[29] In the TGA model (derived from a 15-year-old patient) appreciable less symmetrical flow, with a skewed peak of flow velocity in the ascending aorta, was observed compared with the aortic model of a healthy subject, in which the higher velocities were clustered around the center of the neo-aortic root. In line with the finding of our study, there was a flow jet impingement at the top of the TGA anterior root with a higher WSS in the anterior ascending aortic wall.

In TGA patients, WSS analysis showed in general a more evenly distributed and regionally lower WSS in the dilated root compared with the healthy subjects and clear areas of higher WSS at the right and anterior aortic wall regions from the mid-aortic level and above. The

displacement of flow away from the aortic centerline and directed more towards the vessel wall in the proximal ascending aorta, together with a sudden change in vessel geometry at mid-ascending aortic level, most likely causes an increase in velocity with a higher near-wall velocity gradient resulting in elevated WSS in the right and anterior wall regions of the distal AAo.

The geometric shape of the aorta with its typical appearance after ASO has proved to be one of the most influential factors on blood flow and WSS in aortic flow simulations.[30] The CFD investigation on TGA models after ASO about the influence of geometric changes in the thoracic aorta on the blood flow and WSS reported a large curvature near the aortic root as a distinctive characteristic of the post-ASO geometry.[30] The WSS assessment in the TGA aortic models of that study revealed significantly higher maximum WSS values than in the healthy aortic model, comparable with the findings in this study. The maximum WSS was located in either the ascending aorta or the aortic arch, depending on the degree of aortic torsion and curvature of the two assessed TGA models.[30] The relationship between the degree of aortic diameter reduction at mid-AAo level and WSS in the anterior regions of the distal ascending aorta found in our study supports the hypothesis that in TGA patients after ASO aortic blood flow physiology (expressed in advanced hemodynamic parameters) is altered due to a changed geometry.

Currently, no cases have been documented with aortic rupture or dissection after ASO, but in several re-operated patients the anterior wall of the aneurysmatic aorta was observed to be paper-thin and fragile.[21, 22] These regions correspond to the areas of elevated WSS, as found in our study, and the combined CFD and *in vitro* 4D flow study by Biglino et al.[29] Whether this hemodynamic parameter may add to the prediction of progressive aortic dilatation, aortic wall thinning, or imply a higher lifetime risk on adverse aortic events (aortic rupture or dissection) at that site is unknown and requires further longitudinal follow-up. This is of high importance as, to date, indications for reoperation for neo-aortic root dilatation after ASO to prevent rupture, dissection or progressive neo-aortic regurgitation are unclear. Moreover, extending knowledge on pathophysiologic mechanisms of altered flow hemodynamics on disease progression is necessary, to get better insight and to think about alternative surgical techniques solving long-term residual sequelae in patients with TGA. In this regard, an alternative surgical technique has been described for TGA which preserves a more physiologic spiral anatomy of the great arteries, without applying Lecompte maneuver.[31] Although not frequently applied worldwide and technically not applicable for every TGA patient, results from *in vivo* 4D flow studies in these patients 20 years after ASO reported more physiological aortic blood flow in the great arteries compared with patients who underwent a Lecompte procedure during ASO.[32] These results, together with the results of this study, in which we showed already the presence of abnormal aortic flow hemodynamics in young patients after ASO, suggest aortic geometry as an important factor for altered flow hemodynamics. Although aortic geometry seems to contribute to altered flow hemodynamics, due to the measurements at a single timepoint, it is unknown if the altered FD and WSS are the result of progressive aortic dilatation, or if in any way these

altered hemodynamics were causative to the dilatation. Additional 4D flow studies evaluating the interindividual differences in aortic hemodynamics between TGA patients with different anatomy (i.e. with or without VSD, with different spatial position of the great arteries) and between TGA patients with different surgical ASO techniques (i.e. with and without Lecompte maneuver) need to be performed to optimize management strategies for the best long-term outcomes.

The current study is subject to some limitations. Healthy subjects who were used as a reference group were older compared with the TGA patients included in this study. This might have an impact on the Z-scores that were somewhat larger than expected in the healthy subjects group by the use of the MRI-derived normative data with an age range up to 20 years.[19] While the MRI-derived normative dataset is based on a small population of children and uses nongated contrast-enhanced MRA images, there is currently no larger combined pediatric and adolescent MRI-specific database and this method of normalization is the best available alternative. In addition, the velocity of the aortic flow will decrease with increasing age,[33] which could have lowered the WSS results in healthy subjects, as WSS is closely related to velocity since it is a derivative of velocity.[34, 35] However, the relative small age difference between the adolescent TGA patient group and the healthy young adult subjects is not expected to lead to large differences in mean velocity according to the study on the distribution of velocity in the normal aorta over age by Garcia et al.[33] Therefore, only small differences in WSS are to be expected based on the age difference. These differences do not exceed the WSS differences that have been found between younger TGA patients and healthy subjects, neither will they explain the WSS asymmetry results in this study. Moreover, in healthy adolescents and young adults flow velocity distribution descriptors indicating velocity symmetry and shape (i.e. skewness and kurtosis) only started to increase significantly beyond the age of 40 years.[33] Hence, small differences in age between TGA patients and the healthy control group in this study will not have affected normalized FD measures.

Because of the limited spatial resolution of 4D flow MRI, WSS is known to be underestimated. However, all MR acquisitions in both TGA and healthy subjects were made at the same MR scanner with the same imaging parameters, so differences between groups remain useful. Moreover, patients were analyzed with the software for which a 3D WSS reproducibility analysis study showed robustness of the segmentation and WSS analysis method.[16] Furthermore, the robustness and reproducibility of 2D WSS analysis in cross-sectional planes has been previously demonstrated.[36] However, WSS determination in the neo-aortic root remains a challenge because of the aortic motion and the presence of slow and recirculating flow. Although we did perform a time-resolved segmentation method to account for aortic motion,[16] small border errors may be present for the calculated WSS in the neo-aortic root region, implying that it may not actually reflect the stress on the wall.

In conclusion, TGA patients after ASO have more flow asymmetry in the proximal AAo evidenced by a higher magnitude and directionality of FD, related to increased proximal AAo Z-scores. TGA-specific geometry related to the ASO, with neo-aortic root dilatation and

a sudden change in vessel diameter at mid-AAo level, leads to specific WSS distribution along the AAo in TGA patients that is different with higher WSS compared with healthy subjects. Our observations only start to unravel the interaction between the post-ASO geometry and hemodynamics within the ascending aorta and how the hemodynamics may be involved in the (progression of) neo-aortic root dilatation. Therefore, longitudinal follow-up studies are needed for correlation between changes in systolic WSS and progression of dilatation and to assess the consequence of the increased WSS and its WSS extent on the distal AAo.

References

1. Jatene AD, Fontes VF, Paulista PP, de Souza LC, Neger F, Galantier M, Souza JE. Successful anatomic correction of transposition of the great vessels. A preliminary report. *Arq Bras Cardiol*. 1975;28(4):461-64.
2. Shepard CW, Germanakis I, White MT, Powell AJ, Co-Vu J, Geva T. Cardiovascular Magnetic Resonance Findings Late After the Arterial Switch Operation. *Circ Cardiovasc Imaging*. 2016;9(9).
3. van der Palen RLF, van der Bom T, Dekker A, Tsonaka R, van Geloven N, Kuipers IM, Konings TC, Rammeloo LAJ, Ten Harkel ADJ, Jongbloed MRM, et al. Progression of aortic root dilatation and aortic valve regurgitation after the arterial switch operation. *Heart*. 2019;105(22):1732-40.
4. Geiger J, Hirtler D, Burk J, Stiller B, Arnold R, Jung B, Langer M, Markl M. Postoperative pulmonary and aortic 3D haemodynamics in patients after repair of transposition of the great arteries. *Eur Radiol*. 2014;24(1):200-8.
5. Ntsinjana HN, Capelli C, Biglino G, Cook AC, Tann O, Derrick G, Taylor AM, Schievano S. 3D morphometric analysis of the arterial switch operation using in vivo MRI data. *Clin Anat*. 2014;27(8):1212-22.
6. Dyverfeldt P, Bissell M, Barker AJ, Bolger AF, Carlhall CJ, Ebbers T, Francios CJ, Frydrychowicz A, Geiger J, Giese D, et al. 4D flow cardiovascular magnetic resonance consensus statement. *J Cardiovasc Magn Reson*. 2015;17:72.
7. Frydrychowicz A, Markl M, Hirtler D, Harloff A, Schlensak C, Geiger J, Stiller B, Arnold R. Aortic hemodynamics in patients with and without repair of aortic coarctation: in vivo analysis by 4D flow-sensitive magnetic resonance imaging. *Invest Radiol*. 2011;46(5):317-25.
8. van der Palen RL, Barker AJ, Bollache E, Garcia J, Rose MJ, van Ooij P, Young LT, Roest AA, Markl M, Robinson JD, et al. Altered aortic 3D hemodynamics and geometry in pediatric Marfan syndrome patients. *J Cardiovasc Magn Reson*. 2017;19(1):30.
9. van Ooij P, Markl M, Collins JD, Carr JC, Rigsby C, Bonow RO, Malaisrie SC, McCarthy PM, Fedak PWM, Barker AJ. Aortic Valve Stenosis Alters Expression of Regional Aortic Wall Shear Stress: New Insights From a 4-Dimensional Flow Magnetic Resonance Imaging Study of 571 Subjects. *J Am Heart Assoc*. 2017;6(9).
10. Bissell MM, Hess AT, Biasiolli L, Glaze SJ, Loudon M, Pitcher A, Davis A, Prendergast B, Markl M, Barker AJ, et al. Aortic dilation in bicuspid aortic valve disease: flow pattern is a major contributor and differs with valve fusion type. *Circ Cardiovasc Imaging*. 2013;6(4):499-507.
11. Mahadevia R, Barker AJ, Schnell S, Entezari P, Kansal P, Fedak PW, Malaisrie SC, McCarthy P, Collins J, Carr J, et al. Bicuspid aortic cusp fusion morphology alters aortic three-dimensional outflow patterns, wall shear stress, and expression of aortopathy. *Circulation*. 2014;129(6):673-82.
12. Burris NS, Sigovan M, Knauer HA, Tseng EE, Saloner D, Hope MD. Systolic flow displacement correlates with future ascending aortic growth in patients with bicuspid aortic valves undergoing magnetic resonance surveillance. *Invest Radiol*. 2014;49(10):635-9.
13. Guzzardi DG, Barker AJ, van Ooij P, Malaisrie SC, Puthumana JJ, Belke DD, Mewhort HE, Svystonyuk DA, Kang S, Verma S, et al. Valve-Related Hemodynamics Mediate Human Bicuspid Aortopathy: Insights From Wall Shear Stress Mapping. *J Am Coll Cardiol*. 2015;66(8):892-900.
14. Boussel L, Rayz V, McCulloch C, Martin A, Acevedo-Bolton G, Lawton M, Higashida R, Smith WS, Young WL, Saloner D. Aneurysm growth occurs at region of low wall shear stress: patient-specific correlation of hemodynamics and growth in a longitudinal study. *Stroke*. 2008;39(11):2997-3002.
15. Burk J, Blanke P, Stankovic Z, Barker A, Russe M, Geiger J, Frydrychowicz A, Langer M, Markl M. Evaluation of 3D blood flow patterns and wall shear stress in the normal and dilated thoracic aorta using flow-sensitive 4D CMR. *J Cardiovasc Magn Reson*. 2012;14:84.
16. van der Palen RLF, Roest AAW, van den Boogaard PJ, de Roos A, Blom NA, Westenberg JJM. Scan-rescan reproducibility of segmental aortic wall shear stress as assessed by phase-specific segmentation with 4D flow MRI in healthy volunteers. *MAGMA*. 2018;31(5):653-63.

17. van Kesteren F, Elattar MA, van Lienden KP, Baan J, Jr., Marquering HA, Planken RN. Non-contrast enhanced navigator-gated balanced steady state free precession magnetic resonance angiography as a preferred magnetic resonance technique for assessment of the thoracic aorta. *Clin Radiol*. 2017;72(8):695 e1- e6.

18. Hiratzka LF, Bakris GL, Beckman JA, Bersin RM, Carr VF, Casey DE, Jr., Eagle KA, Hermann LK, Isselbacher EM, Kazerooni EA, et al. 2010 ACCF/AHA/AATS/ACR/ASA/SCA/SCAI/SIR/STS/SVM Guidelines for the diagnosis and management of patients with thoracic aortic disease. A Report of the American College of Cardiology Foundation/American Heart Association Task Force on Practice Guidelines, American Association for Thoracic Surgery, American College of Radiology, American Stroke Association, Society of Cardiovascular Anesthesiologists, Society for Cardiovascular Angiography and Interventions, Society of Interventional Radiology, Society of Thoracic Surgeons,and Society for Vascular Medicine. *J Am Coll Cardiol*. 2010;55(14):e27-e129.

19. Kaiser T, Kellenberger CJ, Albisetti M, Bergstrasser E, Valsangiacomo Buechel ER. Normal values for aortic diameters in children and adolescents--assessment in vivo by contrast-enhanced CMR-angiography. *J Cardiovasc Magn Reson*. 2008;10:56.

20. Sigovan M, Hope MD, Dyverfeldt P, Saloner D. Comparison of four-dimensional flow parameters for quantification of flow eccentricity in the ascending aorta. *J Magn Reson Imaging*. 2011;34(5):1226-30.

21. Koolbergen DR, Manshanden JS, Yazdanbakhsh AP, Bouma BJ, Blom NA, de Mol BA, Mulder BJ, Hazekamp MG. Reoperation for neoaortic root pathology after the arterial switch operation. *Eur J Cardiothorac Surg*. 2014;46(3):474-9.

22. Vida VL, Zanotto L, Zanotto L, Stellin G, European Congenital Heart Surgeons Association Study G, Padalino M, Sarris G, Protopapas E, Prospero C, Pizarro C, et al. Left-Sided Reoperations After Arterial Switch Operation: A European Multicenter Study. *Ann Thorac Surg*. 2017;104(3):899-906.

23. van der Bom T, van der Palen RL, Bouma BJ, van Veldhuisen SL, Vliegen HW, Konings TC, Zwinderman AH, Blom NA, Koolbergen DR, Hazekamp MG, et al. Persistent neo-aortic growth during adulthood in patients after an arterial switch operation. *Heart*. 2014;100(17):1360-5.

24. Jhang WK, Shin HJ, Park JJ, Yun TJ, Kim YH, Ko JK, Park IS, Seo DM. The importance of neo-aortic root geometry in the arterial switch operation with the trap-door technique in the subsequent development of aortic valve regurgitation. *Eur J Cardiothorac Surg*. 2012;42(5):794-9.

25. Lalezari S, Mahtab EA, Bartelings MM, Wisse LJ, Hazekamp MG, Gittenberger-de Groot AC. The outflow tract in transposition of the great arteries: an anatomic and morphologic study. *Ann Thorac Surg*. 2009;88(4):1300-5.

26. van der Palen RLF, van der Zee C, Vink AS, Knobbe I, Jurgens SJ, van Leeuwen E, Bax CJ, du Marchie Sarvaas GJ, Blom NA, Haak MC, et al. Transposition of the great arteries: Fetal pulmonary valve growth and postoperative neo-aortic root dilatation. *Prenat Diagn*. 2019;39(12):1054-63.

27. Raghav V, Barker AJ, Mangiameli D, Mirabella L, Markl M, Yoganathan AP. Valve mediated hemodynamics and their association with distal ascending aortic diameter in bicuspid aortic valve subjects. *J Magn Reson Imaging*. 2018;47(1):246-54.

28. Martins D, Khraiche D, Legendre A, Boddaert N, Raisky O, Bonnet D, Raimondi F. Aortic angle is associated with neo-aortic root dilatation and regurgitation following arterial switch operation. *Int J Cardiol*. 2019;280:53-6.

29. Biglino G, Cosentino D, Steeden JA, De Nova L, Castelli M, Ntsinjana H, Pennati G, Taylor AM, Schievano S. Using 4D Cardiovascular Magnetic Resonance Imaging to Validate Computational Fluid Dynamics: A Case Study. *Front Pediatr*. 2015;3:107.

30. Fukui T, Asama H, Kimura M, Itoi T, Morinishi K. Influence of Geometric Changes in the Thoracic Aorta due to Arterial Switch Operations on the Wall Shear Stress Distribution. *Open Biomed Eng J*. 2017;11:9-16.

31. Chiu IS, Wu SJ, Chen MR, Lee ML, Wu MH, Wang JK, Lue HC. Modified arterial switch operation by spiral reconstruction of the great arteries in transposition. *Ann Thorac Surg*. 2000;69(6):1887-92.

32. Rickers C, Kheradvar A, Sievers HH, Falahatpisheh A, Wegner P, Gabbert D, Jerosch-Herold M, Hart C, Voges I, Putman LM, et al. Is the Lecompte technique the last word on transposition of the great arteries repair for all patients? A magnetic resonance imaging study including a spiral technique two decades postoperatively. *Interact Cardiovasc Thorac Surg*. 2016;22(6):817-25.

33. Garcia J, van der Palen RLF, Bollache E, Jarvis K, Rose MJ, Barker AJ, Collins JD, Carr JC, Robinson J, Rigsby CK, et al. Distribution of blood flow velocity in the normal aorta: Effect of age and gender. *J Magn Reson Imaging*. 2018;47(2):487-98.

34. Allen BD, van Ooij P, Barker AJ, Carr M, Gabbour M, Schnell S, Jarvis KB, Carr JC, Markl M, Rigsby C, et al. Thoracic aorta 3D hemodynamics in pediatric and young adult patients with bicuspid aortic valve. *J Magn Reson Imaging*. 2015;42(4):954-63.

35. van Ooij P, Garcia J, Potters WV, Malaisrie SC, Collins JD, Carr JC, Markl M, Barker AJ. Age-related changes in aortic 3D blood flow velocities and wall shear stress: Implications for the identification of altered hemodynamics in patients with aortic valve disease. *J Magn Reson Imaging*. 2016;43(5):1239-49.

36. Markl M, Wallis W, Harloff A. Reproducibility of flow and wall shear stress analysis using flow-sensitive four-dimensional MRI. *J Magn Reson Imaging*. 2011;33(4):988-94.